

available at [www.sciencedirect.com](http://www.sciencedirect.com)journal homepage: [www.elsevier.com/locate/biochempharm](http://www.elsevier.com/locate/biochempharm)

## Inhibition of 6-hydroxydopamine-induced oxidative damage by 4,5-dihydro-3H-2-benzazepine N-oxides

Ramón Soto-Otero<sup>a</sup>, Estefanía Méndez-Álvarez<sup>a</sup>, Sofía Sánchez-Iglesias<sup>a</sup>,  
Fedor I. Zubkov<sup>b</sup>, Leonid G. Voskressensky<sup>b</sup>, Alexey V. Varlamov<sup>b</sup>,  
Modesto de Candia<sup>c</sup>, Cosimo Altomare<sup>c,\*</sup>

<sup>a</sup> Departamento de Bioquímica y Biología Molecular, Facultad de Medicina, Universidad de Santiago de Compostela, Santiago de Compostela, Spain

<sup>b</sup> Organic Chemistry Department of the Russian Peoples Friendship University, Moscow, Russia

<sup>c</sup> Dipartimento Farmaco-chimico, Facoltà di Farmacia, Università degli Studi di Bari, Via E. Orabona 4, I-70125 Bari, Italy

### ARTICLE INFO

#### Article history:

Received 10 October 2007

Accepted 31 December 2007

#### Keywords:

2-Benzazepine nitrones  
Neuroprotection  
Radical scavengers  
6-Hydroxydopamine  
Lipid peroxidation  
Protein carbonylation

### ABSTRACT

A number of new analogs of 3,3-dimethyl-4,5-dihydro-3H-2-benzazepine 2-oxide, structurally related to the nitron spin trap  $\alpha$ -phenyl-N-tert-butyl nitron (PBN), were synthesized and evaluated for their activity in vitro as protectants against oxidative stress induced in rat brain mitochondria by 6-hydroxydopamine (6-OHDA), a neurotoxin producing experimental model of Parkinson's disease (PD). As assessed by a fluorimetric assay, all 2-benzazepine-based nitrones were shown to decrease hydroxyl radicals ( $\cdot\text{OH}$ ) generated during 6-OHDA autoxidation. The inhibition effects on the  $\cdot\text{OH}$  formation shown by the 5-*gem*-dimethyl derivatives, 2–4 times higher than those of the corresponding 5-methyl derivatives, were attributed to the flattening effect of the 5-*gem*-dimethyl group on the azepine ring, which should enhance nitron reactivity and/or increase stability of the radical adducts. In contrast, owing to steric hindrance, a methyl group to C-1 diminishes the  $\cdot\text{OH}$ -scavenging activity of the nitron group. All the assayed compounds were more potent than PBN as inhibitors of 6-OHDA-induced lipid peroxidation (LPO) and protein carbonylation (PCO), taken as an indicator of mitochondrial protein oxidative damage. The most promising antioxidant (compound 11), bearing 5-*gem*-dimethyl and spiro C-3 cyclohexyl groups, highlighted in this study as the best features, inhibited LPO and PCO with  $\text{IC}_{50}$  values of 20 and 48  $\mu\text{M}$ , respectively, showing a potency improvement over PBN of two order magnitude. Both LPO and PCO inhibition potency data were found primarily related to the  $\cdot\text{OH}$ -scavenging activities, whereas lipophilicity plays a role in improving the LPO (but not PCO) inhibition, as a statistically valuable two-parameter equation proved.

© 2008 Elsevier Inc. All rights reserved.

\* Corresponding author. Tel.: +39 080 5442781; fax: +39 080 5442230.

E-mail address: [altomare@farmchim.uniba.it](mailto:altomare@farmchim.uniba.it) (C. Altomare).

Abbreviations: PD, Parkinson's disease; AD, Alzheimer's disease; ALS, amyotrophic lateral sclerosis; 6-OHDA, 6-hydroxydopamine; MPTP, N-methyl-4-phenyl-1,2,3,6-tetrahydropyridine; PBN,  $\alpha$ -phenyl-N-tert-butyl nitron; ROS, reactive oxygen species;  $\cdot\text{OH}$ , hydroxyl radical; LPO, lipid peroxidation; RCS, reactive carbonyl species; PCO, protein carbonylation; THA, terephthalic acid; TBA, thiobarbituric acid; TBARS, thiobarbituric acid reactive substances; TCA, trichloroacetic acid; MDA, malondialdehyde; MAO, monoamine oxidase; BSA, bovine serum albumin; SDS, sodium dodecylsulfate.

0006-2952/\$ – see front matter © 2008 Elsevier Inc. All rights reserved.

doi:10.1016/j.bcp.2007.12.010

## 1. Introduction

Free radical-induced oxidation of cell macromolecules (lipids, proteins, DNA, etc.) is implicated in several human pathogenic processes, including cardiovascular diseases (e.g., stroke, atherosclerosis) [1] and inflammatory (e.g., rheumatoid arthritis) [2]. Over the last two decades, significant accumulating evidence has also shown that generation of reactive oxygen species (ROS) and oxidative damage in the central nervous system (CNS) are major events occurring in Parkinson's disease (PD) [3] and other neurodegenerative disorders, such as Alzheimer's disease (AD) and amyotrophic lateral sclerosis (ALS), as well as in aging processes [4]. Despite a large body of biochemical data gathered from human brain autopsy studies, the cause of neurodegeneration in PD has not yet been completely established. Nevertheless, animal models, based on the toxic damage induced by the neurotoxins 6-hydroxydopamine (6-OHDA) [5], N-methyl-4-phenyl-1,2,3,6-tetrahydropyridine (MPTP) [6] and related compounds [7,8], have shown that iron-dependent oxidative stress, increased levels of iron and monoamine oxidase (MAO)-B activity and depletion of antioxidants (e.g., glutathione, GSH) play major roles in PD. Indeed, antioxidants, monoamine oxidase (MAO)-B inhibitors and iron chelators, have shown neuroprotective effects in animal models either *in vitro* and *in vivo* [9–13], but unfortunately they failed in the PD human therapy [3] when administered as single drugs.

6-OHDA, used in this and previous studies [14] for inducing oxidative stress associated with the PD-related dopaminergic neuron loss, is readily autoxidized and oxidatively deaminated by MAO, yielding hydrogen peroxide ( $H_2O_2$ ) and the corresponding *p*-quinone.  $H_2O_2$  may generate the most reactive ROS, that is hydroxyl radicals ( $\cdot OH$ ) [15], and, ultimately, lipid-derived carbon- and oxygen-centered radicals, as lipid peroxidation (LPO) products. In turn, 6-OHDA quinone triggers a cascade of oxidative reactions finally resulting in the formation of an insoluble polymeric pigment related to neuromelanin [16,17]. It has also been reported that 6-OHDA inhibits complexes I and IV of the mitochondrial respiratory chain [18,19]. The oxidative stress caused by  $\cdot OH$  generated during 6-OHDA autoxidation is suggested as a major causal factor of its neurotoxicity [20].

Proteins are major targets for ROS and secondary by-products of oxidative stress, and ROS-induced protein modifications can lead to unfolding or alteration of protein

structure. Protein carbonylation (PCO) is an irreversible oxidative damage, that often leads to formation of high-molecular-weight aggregates, which are resistant to degradation and accumulated as damaged or unfolded proteins [21]. PCO can take place through different oxidative pathways. ROS can react (i) directly with the protein, or (ii) with molecules, such as sugars and lipids, generating in turn reactive carbonyl species (RCS), which then react with protein. RCS, generated by peroxidation of polyunsaturated fatty acids, induce PCO, playing a major role in the etiology and/or progression of several human illnesses, including neurodegenerative disorders associated with the deposition of protein aggregates in tissues [22,23]. Some proteins are more susceptible than others to oxidative stress. For example, human brain copper–zinc superoxide dismutase (SOD1) has been proven to be a major target of oxidative damage in PD and AD [24].

In the last decade, nitron spin traps,  $\alpha$ -phenyl-N-tert-butyl nitron (PBN) and structurally related compounds (Fig. 1), which react covalently with short-lived free radicals, such as  $\cdot OH$ , have shown efficacy in a variety of animal models of CNS injury [25–27], proving to be effective in ischemic stroke models (especially the PBN disodium 1,3-disulfonate salt derivative, NXY-059) [28] and aging [29,30]. Incorporating the nitron functionality in a ring (cyclic PBN analogs) did strongly increase potency relative to PBN against oxidative injury and cell toxicity, as a result of favorable changes in the HOMO/LUMO energy levels and greater accessibility of the nitron double bond [26,31–34]. A number of 3,3-dimethyl-3,4-dihydroisoquinoline 2-oxides (1, Fig. 1), 3,3-dimethyl-4,5-dihydro-3H-2-benzazepine 2-oxides (2), and their spiro C-3 cycloalkyl analogs, have been found out as inhibitors of LPO. Electron spin resonance (ESR) spectroscopy has clearly demonstrated that cyclic nitrones 1 and 2 are able to trap radicals, forming more stable spin adducts than PBN [33,34]. In particular, chloro-substituted 2-benzazepine nitrones (2, X = 8-Cl or 7,9-(Cl)<sub>2</sub>) proved to be potent radical scavengers in both lipid and apoprotein fractions of low density lipoproteins [33]. Moreover, structure–activity relationship (SAR) studies have highlighted the following main factors increasing their *in vitro* inhibitory potency: (i) the presence of a second antioxidant functionality, such as *o,o'*-dimethylphenol (e.g., X = 6,8-(CH<sub>3</sub>)<sub>2</sub>-7-OH in 2); (ii) lipophilicity increments, as resulted from expansion of the nitron-containing ring (2-benzazepine versus isoquinoline), replacement of the *gem*-dimethyl group

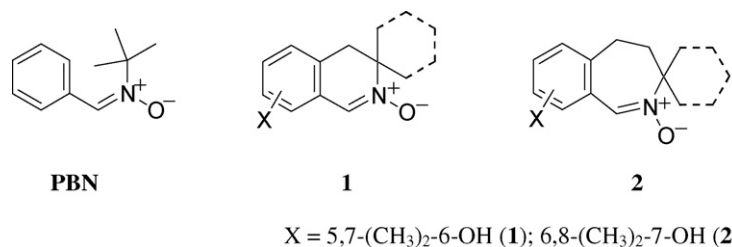
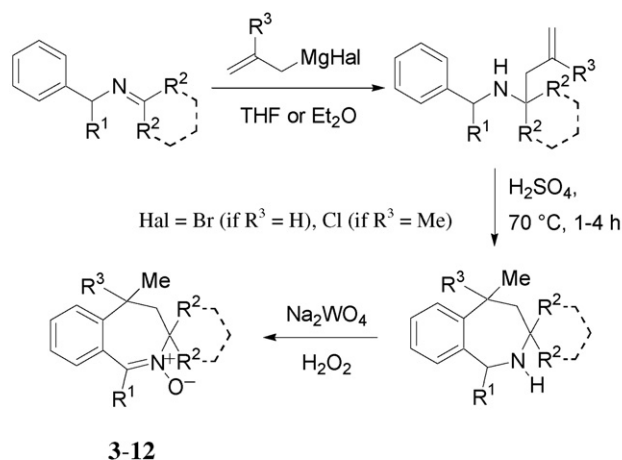


**Fig. 1** – Structures of PBN spin trap and structurally related cyclic nitrones. The structures of 3,3-dimethyl-3,4-dihydroisoquinoline 2-oxides (1), 3,3-dimethyl-4,5-dihydro-3H-2-benzazepine 2-oxides (2), and their spiro C-3 cycloalkyl analogs, are shown, along with benzene ring X-substitution which proved to achieve significant improvements in activity over the parent compounds (X = H).



	<b>3</b>	<b>4</b>	<b>5</b>	<b>6</b>	<b>7</b>	<b>8</b>	<b>9</b>	<b>10</b>	<b>11</b>	<b>12</b>
R <sup>1</sup>	H	H	Me	Me	Ph	H	H	H	H	Me
R <sup>2</sup>	Me	Me	Me	Me	Me	Me, Et	(CH <sub>2</sub> ) <sub>4</sub>	(CH <sub>2</sub> ) <sub>5</sub>	(CH <sub>2</sub> ) <sub>5</sub>	(CH <sub>2</sub> ) <sub>5</sub>
R <sup>3</sup>	H	Me	H	Me	Me	Me	H	H	Me	H

**Fig. 2 – Scheme of synthesis and structures of the examined 2-benzazepine nitrones.**

at the C-3 position with a spirocyclohexyl moiety and/or hydrophobic X substituents on the fused benzene ring.

Recently, we have prepared a number of 2-benzazepine nitron congeners (compounds 3–12) through an efficient synthesis (Fig. 2) [35] and studied their neuroprotective properties, as assessed by the ability to scavenge <sup>•</sup>OH, generated during 6-OHDA autoxidation, and to inhibit 6-OHDA-induced lipid peroxide formation (LPO), as assessed by monitoring the formation of thiobarbituric acid reactive substances (TBARS), and protein oxidative damage, as indicated by the increase of protein carbonyl content, in rat brain mitochondria. Herein we report the results from this neurobiological investigation, followed by SAR to analyze the data. Chiral compounds 3, 5, 8–10 and 12 were tested as racemic mixtures, the investigation of enantioselective effects being out of the scope of this work.

## 2. Materials and methods

### 2.1. Chemicals

PBN, 6-OHDA hydrobromide, terephthalic acid, thiobarbituric acid, butylated hydroxytoluene crystalline, 2,4-dinitrophenylhydrazine hydrochloride, desferrioxamine, 1,1,3,3-tetraethoxypropane, 5,5'-dithiobis-(2-nitrobenzoic acid), sodium dodecylsulfate (SDS), EDTA, and bovine serum albumin (BSA) were purchased from Sigma Chemical Co. (St. Louis, MO, USA). Guanidine hydrochloride was purchased from Aldrich Chemical Co. (Milwaukee, WI, USA). The water used for the preparations of solutions was of 18.2 MΩ (Milli-RiOs/Q-A10 grade, Millipore Corp., Bedford, MA, USA). All remaining

chemicals used were of analytical grade and were purchased from Fluka Chemie AG (Buchs, Switzerland).

### 2.2. Synthesis of 4,5-dihydro-3H-2-benzazepine N-oxide derivatives

3,3-Dimethyl-4,5-dihydro-3H-2-benzazepine N-oxide derivatives and their spiro C-3-cycloalkane analogs were prepared through an efficient synthesis reported by some of us [35]. First, 2,3,4,5-tetrahydro-1H-2-benzazepines were easily synthesized in two steps from readily available imines. They were then converted, with moderate-to-high yields, into the 2-benzazepine nitrones via hydrogen peroxide oxidation in the presence of catalytic amounts of sodium tungstate, under mild conditions. 5-Methyl-4,5-dihydrospiro[2-benzazepine-3,1'-cyclopentane] 2-oxide (9), 5-methyl-4,5-dihydrospiro[2-benzazepine-3,1'-cyclohexane] 2-oxide (10), and 1,5-dimethyl-4,5-dihydrospiro[2-benzazepine-3,1'-cyclohexane] 2-oxide (12) have been reported earlier [35]. Compounds 4, 9 and 12 were prepared and tested as hydrochlorides.

#### 2.2.1. Homoallylamines

2-Methyl-N-(phenylmethyl)pent-4-en-2-amine (for 3), 2,4-dimethyl-N-(phenylmethyl)pent-4-en-2-amine (for 4), 2-methyl-N-(1-phenylethyl)pent-4-en-2-amine (for 5), 2,4-dimethyl-N-(1-phenylethyl)pent-4-en-2-amine (for 6), N-(diphenylmethyl)-2,4-dimethylpent-4-en-2-amine (for 7), 3,5-dimethyl-N-(phenylmethyl)hex-5-en-3-amine (for 8), and 1-(2-methylprop-2-en-1-yl)-N-(phenylmethyl)cyclohexanamine (for 11) were obtained according to reported procedures [36–38] from the corresponding imines and allyl(methyl) magnesium bromide.

### 2.2.2. 2,3,4,5-Tetrahydro-1H-2-benzazepine

3,3,5-Trimethyl-2,3,4,5-tetrahydro-1H-2-benzazepine (for 3), 3,3,5,5-tetramethyl-2,3,4,5-tetrahydro-1H-2-benzazepine (for 4), 1,3,3,5-tetramethyl-2,3,4,5-tetrahydro-1H-2-benzazepine (for 5), 1,3,3,5,5-pentamethyl-2,3,4,5-tetrahydro-1H-2-benzazepine (for 6), 3,3,5,5-tetramethyl-1-phenyl-2,3,4,5-tetrahydro-1H-2-benzazepine (for 7), 3-ethyl-3,5,5-trimethyl-2,3,4,5-tetrahydro-1H-2-benzazepine (for 8), and 5,5-dimethyl-1,2,4,5-tetrahydrospiro[2-benzazepine-3,1'-cyclohexane] (for 11) were obtained according to already described methods [31,39]. Selected spectral and physical data for 2-benzazepines are given below.

2.2.2.1. 3,3,5,5-Tetramethyl-2,3,4,5-tetrahydro-1H-2-benzazepine (for 4). Pale-yellow oil, 55% yield. bp 104–7 °C/2 torr; <sup>1</sup>H NMR (CDCl<sub>3</sub>, 400 MHz) δ 1.22 (s, 6H), 1.41 (s, 6H), 1.43 (br. s, 1H), 1.81 (d, J = 14.9 Hz, 1H), 1.82 (d, J = 14.9 Hz, 1H), 4.03 (s, 2H), 7.01 (dd, J = 7.6, 2.1 Hz, 1H), 7.06 (dt, J = 7.6, 2.6 Hz, 1H), 7.17 (dt, J = 7.6, 2.1 Hz, 1H), 7.34 (dd, J = 7.6, 2.6 Hz, 1H) ppm; ESI-MS *m/z*: 204 (MH)<sup>+</sup>. Anal. Calcd. for C<sub>14</sub>H<sub>21</sub>N: C, 82.70; H, 10.41; N, 6.89. Found: C, 82.76; H, 10.34; N, 6.90.

2.2.2.2. 1,3,3,5-Tetramethyl-2,3,4,5-tetrahydro-1H-2-benzazepine (for 5). Colourless oil, 42% yield. bp 100–1 °C/3 torr; isomer ratio 1:1.5, <sup>1</sup>H NMR (CDCl<sub>3</sub>, 400 MHz), major isomer: δ 1.06 (s, 3H), 1.26 (dd, J = 13.9, 11.5 Hz, 1H), 1.39 (s, 3H), 1.40 (d, J = 7.3 Hz, 3H), 1.54 (d, J = 6.8 Hz, 3H), 1.60 (d, J = 13.9 Hz, 1H), 3.37 (dq, J = 11.5, 7.3 Hz, 1H), 7.19–7.34 (m, 4H) ppm; minor isomer: δ 1.15 (s, 3H), 1.17 (s, 3H), 1.41 (d, J = 7.3 Hz, 3H), 1.53 (d, J = 6.8 Hz, 3H), 1.74 (dd, J = 13.9, 10.3 Hz, 1H), 1.83 (dd, J = 13.9, 3.7 Hz, 1H), 3.43 (m, J = 10.3, 7.3, 3.7 Hz, 1H), 4.41 (q, J = 6.8 Hz, 1H), 7.19–7.34 (m, 4H) ppm; ESI-MS *m/z*: 204 (MH)<sup>+</sup>. Anal. Calcd. for C<sub>14</sub>H<sub>21</sub>N: C, 82.70; H, 10.41; N, 6.89. Found: C, 82.66; H, 10.39; N, 6.85.

2.2.2.3. 1,3,3,5,5-Pentamethyl-2,3,4,5-tetrahydro-1H-2-benzazepine (for 6). Pale-yellow oil, 50% yield. bp 103–4 °C/3 torr; <sup>1</sup>H NMR (CDCl<sub>3</sub>, 400 MHz) δ 1.24 (s, 3H), 1.25 (s, 3H), 1.41 (s, 3H), 1.49 (s, 3H), 1.51 (d, J = 6.7 Hz, 3H), 1.60 (d, J = 15.0 Hz, 1H), 2.12 (d, J = 15.0 Hz, 1H), 4.46 (d, J = 6.7 Hz, 1H), 7.15 (dt, J = 7.3, 1.6 Hz, 1H), 7.19 (dt, J = 7.3, 1.6 Hz, 1H), 7.27 (dd, J = 7.3, 1.6 Hz, 1H), 7.38 (dd, J = 7.3, 1.6 Hz, 1H) ppm; ESI-MS *m/z*: 218 (MH)<sup>+</sup>. Anal. Calcd. for C<sub>15</sub>H<sub>23</sub>N: C, 82.89; H, 10.67; N, 6.44. Found: C, 82.95; H, 10.60; N, 6.45.

2.2.2.4. 3-Ethyl-3,5,5-trimethyl-2,3,4,5-tetrahydro-1H-2-benzazepine (for 8). Pale-yellow oil, 66% yield. bp 131–2 °C/5 torr; <sup>1</sup>H NMR (CDCl<sub>3</sub>, 400 MHz) δ 0.93 (t, J = 7.3 Hz, 3H), 1.16 (s, 3H), 1.42 (s, 3H), 1.46 (s, 3H), 1.54 (m, 2H), 1.74 (d, J = 15.1 Hz, 1H), 1.86 (d, J = 15.1 Hz, 1H), 4.05 (s, 1H), 7.04 (dd, J = 7.5, 0.9 Hz, 1H), 7.20 (t, J = 7.5, 1.4 Hz, 1H), 7.37 (dd, J = 7.5, 1.4 Hz, 1H), 7.39 (td, J = 7.5, 0.9 Hz, 1H) ppm; ESI-MS *m/z*: 218 (MH)<sup>+</sup>. Anal. Calcd. for C<sub>15</sub>H<sub>23</sub>N: C, 82.89; H, 10.67; N, 6.44. Found: C, 82.92; H, 10.69; N, 6.45.

2.2.2.5. 5,5-Dimethyl-1,2,4,5-tetrahydrospiro[2-benzazepine-3,1'-cyclohexane] (for 11). Viscous yellow oil, 85% yield. bp 139–42 °C/2 torr; <sup>1</sup>H NMR (CDCl<sub>3</sub>, 400 MHz) δ 1.42 (s, 6H), 1.25–1.75 (m, 10H), 1.79 (s, 2H), 4.01 (s, 2H), 6.89–7.35 (m, 4H) ppm; ESI-MS *m/z*: 244 (MH)<sup>+</sup>. Anal. Calcd. for C<sub>17</sub>H<sub>25</sub>N: C, 83.95; H, 10.29; N, 5.76. Found: C, 84.24; H, 9.95; N, 5.81.

### 2.2.3. Oxidation of benz-2-azepines to nitrones (3–8, 11):

#### Typical procedure

To a solution of 50 mmol of benz-2-azepine and Na<sub>2</sub>WO<sub>4</sub>·2H<sub>2</sub>O (0.83 g, 2.5 mmol) in acetone–water mixture (9:1, v/v, 100 mL), 50% H<sub>2</sub>O<sub>2</sub> (12 mL, 200 mmol) was added dropwise at 0 °C (0.5 h). The resulting mixture was stirred at room temperature for 24–96 h (TLC monitoring). After the reaction was completed, the reaction mixture was poured into water (300 mL) and extracted with CH<sub>2</sub>Cl<sub>2</sub> (5 × 30 mL). The combined organic extracts were dried over MgSO<sub>4</sub> and concentrated *in vacuo*. Crystallization of the resulting solids from hexane–ethyl acetate mixture gave white crystals of nitrones (3–8, 11). In case of compounds 3, 5, 8 the oily residues were purified by column chromatography on Al<sub>2</sub>O<sub>3</sub> (using hexane–ethyl acetate, 5:1, v/v, as eluent). Slowly crystallizing nitrones (3, 6, 8, 11) were converted into hydrochlorides by mixing their ether solutions (1 g of nitrone in 50 mL of dry diethyl ether) with saturated HCl/Et<sub>2</sub>O solution until pH 5 was achieved. Resulting white precipitates were filtered-off, washed with absolute ether and dried on air (90–95% yields).

2.2.3.1. 3,3,5-Trimethyl-4,5-dihydro-3H-2-benzazepine 2-oxide (3). White crystals, 75% yield. mp 71–73 °C; <sup>1</sup>H NMR (CDCl<sub>3</sub>, 400 MHz) δ 1.43 (d, J = 7.2 Hz, 3H), 1.53 (s, 3H), 1.65 (s, 3H), 1.99 (dd, J = 1.9, 15.0 Hz, 1H), 2.12 (dd, J = 9.4, 15.0 Hz, 1H), 3.13 (m, 1H), 7.14–7.30 (m, 4H), 7.91 (s, 1H) ppm; EI-MS (70 eV) *m/z* (rel. intensity): 203 (32, M<sup>+</sup>), 144 (16), 132 (100), 131 (26), 130 (28), 129 (16), 128 (19), 115 (29), 104 (37), 77 (22); IR (KBr, ν cm<sup>-1</sup>) 1529 (C=N). Anal. Calcd. for C<sub>13</sub>H<sub>17</sub>NO: C, 76.81; H, 8.43; N, 6.89. Found: C, 76.65; H, 8.51; N, 6.81.

2.2.3.2. 3,3,5,5-Tetramethyl-4,5-dihydro-3H-2-benzazepine 2-oxide (4). White crystals, 55% yield. mp 51–2 °C; <sup>1</sup>H NMR (CDCl<sub>3</sub>, 400 MHz) δ 1.49 (s, 3H), 1.72 (s, 3H), 2.29 (s, 2H), 7.44 (td, J = 7.5, 1.2 Hz, 1H), 7.52 (bd, J = 7.5 Hz, 1H), 7.62–7.71 (m, 2H), 9.09 (s, 1H) ppm; EI-MS (70 eV) *m/z* (rel. intensity): 217 (35, M<sup>+</sup>), 161 (22), 146 (39), 145 (29), 144 (55), 143 (16), 130 (14), 129 (28), 128 (100), 115 (31); IR (KBr, ν cm<sup>-1</sup>) 1545 (C=N). Anal. Calcd. for C<sub>14</sub>H<sub>19</sub>NO: C, 77.38; H, 8.81; N, 6.45. Found: C, 77.42; H, 8.85; N, 6.66.

2.2.3.3. 1,3,3,5-Tetramethyl-4,5-dihydro-3H-2-benzazepine 2-oxide (5). White crystals, 66% yield. mp 69–71 °C; <sup>1</sup>H NMR (CDCl<sub>3</sub>, 400 MHz) δ 0.82 (s, 3H), 1.23 (d, J = 6.8 Hz, 3H), 1.30 (s, 3H), 1.86 (dd, J = 12.2, 14.0 Hz, 1H), 2.30 (s, 3H), 2.45 (dd, J = 6.8, 14.0 Hz, 1H), 2.98 (m, 1H), 7.27–7.31 (m, 4H) ppm; EI-MS (70 eV) *m/z* (rel. intensity): 217 (48, M<sup>+</sup>), 175 (22), 160 (23), 158 (40), 146 (100), 145 (54), 144 (56), 143 (31), 128 (26), 91 (29); IR (KBr, ν cm<sup>-1</sup>) 1542 (C=N). Anal. Calcd. for C<sub>14</sub>H<sub>19</sub>NO: C, 77.38; H, 8.81; N, 6.45. Found: C, 77.52; H, 8.75; N, 6.43.

2.2.3.4. 1,3,3,5,5-Pentamethyl-4,5-dihydro-3H-2-benzazepine 2-oxide (6). White crystals (hydrochloride), 70% yield. mp 165–73 °C; <sup>1</sup>H NMR (CDCl<sub>3</sub>, 400 MHz) δ 1.21 (s, 6H), 1.30 (s, 6H), 2.25 (s, 2H), 2.44 (s, 3H), 7.21–7.30 (m, 1H), 7.28–7.33 (m, 2H), 7.35–7.38 (m, 1H) ppm; EI-MS (70 eV) *m/z* (rel. intensity): 231 (24, M<sup>+</sup>), 160 (59), 159 (22), 158 (100), 157 (19), 144 (18), 143 (20), 129 (19), 128 (29), 115 (21); IR (KBr, ν cm<sup>-1</sup>) 1555 (C=N). Anal. Calcd. for C<sub>15</sub>H<sub>21</sub>NO: C, 77.88; H, 9.15; N, 6.05. Found: C, 77.81; H, 9.30; N, 6.18.

2.2.3.5. 3,3,5,5-Tetramethyl-1-phenyl-4,5-dihydro-3H-2-benzazepine 2-oxide (7). White crystals, 73% yield. mp 97–9 °C; <sup>1</sup>H NMR (CDCl<sub>3</sub>, 400 MHz) δ 1.20 (s, 6H), 1.38 (s, 6H), 2.23 (s, 2H), 7.21–7.73 (m, 9H) ppm; EI-MS (70 eV) *m/z* (rel. intensity): 293 (56, M<sup>+</sup>), 251 (22), 237 (19), 222 (70), 221 (32), 220 (100), 158 (37), 128 (20), 91 (21), 77 (38), 58 (19); IR (KBr, ν cm<sup>-1</sup>) 1540 (C=N). Anal. Calcd. for C<sub>20</sub>H<sub>23</sub>NO: C, 81.87; H, 7.90; N, 4.77. Found: C, 81.97; H, 7.77; N, 4.73.

2.2.3.6. 3-Ethyl-3,5,5-trimethyl-4,5-dihydro-3H-2-benzazepine 2-oxide (8). White crystals, 67% yield. mp 81–2 °C (162–9 °C for hydrochloride); <sup>1</sup>H NMR (CDCl<sub>3</sub>, 400 MHz) δ 0.81 (t, *J* = 7.4 Hz, 3H), 1.3 (s, 3H), 1.44 (s, 3H), 1.58 (s, 3H), 1.71 (qd, *J* = 7.4, 14.4 Hz, 1H), 1.83 (qd, *J* = 7.4, 14.4 Hz, 1H), 2.04 (d, *J* = 15.4 Hz, 1H), 2.27 (d, *J* = 15.4 Hz, 1H), 7.10 (bd, *J* = 7.6 Hz, 1H), 7.20 (td, *J* = 7.6, 1.3 Hz, 1H), 7.26 (td, *J* = 7.6, 1.3 Hz, 1H), 7.33 (bd, *J* = 7.6 Hz, 1H), 7.97 (s, 1H) ppm; EI-MS (70 eV) *m/z* (rel. intensity): 231 (16, M<sup>+</sup>), 214 (17), 202 (80), 186 (29), 162 (55), 160 (12), 145 (100), 144 (56), 143 (30), 130 (35), 129 (57), 128 (38), 115 (33), 91 (17), 77 (13), 41 (10); IR (KBr, ν cm<sup>-1</sup>) 1542 (C=N). Anal. Calcd. for C<sub>15</sub>H<sub>21</sub>NO: C, 77.88; H, 9.15; N, 6.05. Found: C, 77.90; H, 9.21; N, 6.17.

2.2.3.7. 5,5-Dimethyl-4,5-dihydrospiro[2-benzazepine-3,1'-cyclohexane] 2-oxide (11). White crystals (hydrochloride), 50% yield. mp 164–5 °C; <sup>1</sup>H NMR (CDCl<sub>3</sub>, 400 MHz) δ 1.36–1.61 (m, 4H), 1.51 (s, 6H), 1.72–1.90 (m, 4H), 2.33–2.43 (m, 2H), 2.41 (s, 2H), 7.43 (td, *J* = 7.6, 1.3 Hz, 1H), 7.49–7.53 (m, 1H), 7.59–7.66 (m, 2H), 9.13 (s, 1H) ppm; EI-MS (70 eV) *m/z* (rel. intensity): 257 (11, M<sup>+</sup>), 240 (100), 198 (26), 145 (17), 144 (16), 143 (12), 130 (15), 129 (28), 128 (33), 115 (16); IR (KBr, ν cm<sup>-1</sup>) 1586 (C=N). Anal. Calcd. for C<sub>17</sub>H<sub>23</sub>NO: C, 79.33; H, 9.01; N, 5.44. Found: C, 79.28; H, 9.16; N, 5.38.

### 2.3. Preparation of brain mitochondria

All procedures were carried out in accordance with the NIH *Guide for Care and Use of Laboratory Animals*, and were approved by the Animal Ethics Committee of the Universidad de Santiago de Compostela (Santiago de Compostela, Spain). Male Sprague–Dawley rats weighting 250–300 g were used. The rats were received from the breeder (Animalario de la Universidad de Santiago de Compostela) at least 2 days before sacrifice, and were kept at 22 °C, on a 12:12 light–dark schedule, and with *ad libitum* access to food and water. Animals were stunned with carbon dioxide and killed by decapitation. Brains were immediately removed and washed in ice-cold isolation medium (pH 7.4, Na<sub>2</sub>PO<sub>4</sub>/KH<sub>2</sub>PO<sub>4</sub> isotonized with sucrose). Brain mitochondria were then obtained by differential centrifugation with minor modifications to a previously published method [40]. Briefly, after removing blood vessels and pial membranes, the brains were manually homogenized with four volumes (w/v) of the isolation medium. Then, the homogenate was centrifuged in an Avanti J-25 centrifuge (Beckman Instruments, Palo Alto, USA) at 1000 × *g* for 5 min at 4 °C. The supernatant was centrifuged at 12,500 × *g* for 15 min. The mitochondrial pellet was then washed once with isolation medium and recentrifuged under the same conditions. Finally, the mitochondrial pellet was reconstituted in a buffer solution (Na<sub>2</sub>PO<sub>4</sub>/KH<sub>2</sub>PO<sub>4</sub> isotonized with KCl, pH 7.4) and stored in aliquots under liquid nitrogen.

**Table 1 – IC<sub>50</sub> values for inhibition of •OH production during 6-OHDA autoxidation**

Compound	IC <sub>50</sub> (μM)
PBN	782 ± 39
3	48 ± 3.9 <sup>*</sup>
4	17 ± 2.7 <sup>*,§</sup>
5	235 ± 21 <sup>*,§</sup>
6	63 ± 5.0 <sup>*</sup>
7	46 ± 5.0 <sup>*</sup>
8	57 ± 4.2 <sup>*</sup>
9	7 ± 1.2 <sup>*,§</sup>
10	37 ± 2.2 <sup>*</sup>
11	19 ± 2.6 <sup>*,§</sup>
12	278 ± 14 <sup>*,§</sup>

The •OH formation was monitored by fluorimetry using terephthalic acid (THA) as a chemical dosimeter. The IC<sub>50</sub> values, determined using the 10-min time point, represent the concentrations of the test nitrones required to inhibit •OH formation by 50%. Values are means ± S.E.M. from four independent determinations. Statistical significance at *P* < 0.05 (one-way ANOVA and Bonferroni test) was established in comparison with the corresponding control: \*, PBN; §, cmpd 3.

The protein concentration of mitochondrial preparations was determined according to the method of Markwell et al. [41], using BSA as the standard.

### 2.4. Fluorimetric monitoring of hydroxyl radical formation

The hydroxyl radical (•OH) formation was monitored fluorimetrically using a previously reported method [14,40,42,43], in which terephthalic acid (THA) is used as a dosimeter for the detection of •OH *in vitro*. A luminescence spectrometer Model LS50B (Perkin-Elmer, Norwalk, CT, USA) was used. The cuvette holder was thermostatically maintained at 37 °C and the sample continuously stirred with a magnetic stirrer.

A buffer solution (Na<sub>2</sub>PO<sub>4</sub>/KH<sub>2</sub>PO<sub>4</sub> isotonized with KCl, pH 7.4) containing 10 mM terephthalic acid was incubated for 5 min to reach the working temperature. Then, the test 2-benzazepine nitron (final concentration range from 5 μM to 1 mM) or water was incorporated into the incubation followed by addition of either 6-OHDA (10 μM) or 1 mM KCl (pH 2.0). All the reported concentrations are final concentrations in the incubation mixture. Monitoring of •OH formation was immediately initiated and maintained for the subsequent 10 min. The excitation and emission wavelengths used were 312 and 426 nm, respectively. Fluorescence measurements were all relative to the initial reading and the peak of relative fluorescence (Δ*F*<sub>max</sub>) used to express the amount of the produced •OH.

The test compound concentration that inhibited •OH formation by 50% (IC<sub>50</sub>) was calculated using the program Origin<sup>®</sup> v. 6.0 (Microcal Software Inc., Northampton, MA, USA) from a concentration-response curve generated with seven different concentrations of the 2-benzazepine nitron (Table 1).

### 2.5. Lipid peroxidation assay

The inhibitory effects of the test nitrones on the LPO were assessed by monitoring the formation of TBARS, using a slightly modified spectrophotometric method [40].

A brain mitochondrial preparation (1 mg protein/mL), in a  $\text{Na}_2\text{PO}_4/\text{KH}_2\text{PO}_4$  buffer (pH 7.4) isotonized with KCl, was incubated at 37 °C for 5 min to reach the working temperature. Then, the test nitrone (concentrations ranging from 5  $\mu\text{M}$  to 1 mM) or water was incorporated into the incubation, followed by addition of 6-OHDA (10  $\mu\text{M}$ ) or 1 mM KCl (pH 2.0), and the mixture incubated for exactly 20 min. Butylated hydroxytoluene (20  $\mu\text{M}$ ) and desferrioxamine (20  $\mu\text{M}$ ) were immediately added, in order to prevent amplification of the lipid peroxidation during the assay. All the above reported concentrations are final concentrations in the incubation medium.

An aliquot of the sample (200  $\mu\text{L}$ ) was treated with SDS (8.1%, w/v), followed by addition of acetic acid (20%), and the mixture vortexed for 1 min. Then, thiobarbituric acid (TBA, 0.8%) was added and the resulting mixture incubated at 95 °C for 60 min. After cooling to room temperature, 3 mL of *n*-butanol were added and the mixture shaken vigorously. After centrifugation at  $2500 \times g$  for 10 min, the absorbance of the supernatant (organic layer) was measured at 532 nm using an Ultrospec III spectrophotometer (Pharmacia Biotech, Uppsala, Sweden).

For calibration, a standard curve (5–150 nM) was generated using the malondialdehyde (MDA), prepared via acid-catalyzed hydrolysis ( $\text{H}_2\text{SO}_4$ ; 1.5%, v/v) of 1,1,3,3-tetraethoxypropane. The protein concentration of the sample was determined according to a previously reported method [41], using BSA as the standard. The  $\text{IC}_{50}$  values are listed in Table 2.

## 2.6. Assessment of protein carbonyl content

The ability of the examined cyclic nitrones to inhibit the protein oxidative damage caused by the autoxidation of 10  $\mu\text{M}$  6-OHDA in the rat brain mitochondrial preparation was assayed by determining the content of protein carbonyls (PCOs), through a modified published spectrophotometric method [40]. Brain mitochondria (1 mg protein/mL) were incubated in  $\text{Na}_2\text{PO}_4/\text{KH}_2\text{PO}_4$  buffer (pH 7.4, isotonized with KCl), at 37 °C for 5 min. Then, the test nitrone (final concentrations ranging from 5  $\mu\text{M}$  to 1 mM) or water was incorporated into the incubation, followed by 6-OHDA (10  $\mu\text{M}$ ) or 1 mM KCl (pH 2.0), and the mixture incubated for exactly 20 min.

An aliquot of the sample (200  $\mu\text{L}$ ) was then immediately submitted to protein precipitation, by adding of trichloroacetic acid (TCA 20%, w/v), followed by centrifugation at  $15,000 \times g$  for 5 min. The resulting pellet was reconstituted in 0.5 M NaOH with sonication (Branson Sonic Corp., Danbury, CT, USA) for 5 s. Then, 10 mM 2,4-dinitrophenylhydrazine in 2 M chloric acid was added and the mixture incubated at room temperature for 1 h, in darkness with continuous agitation. After the addition of TCA (20%, w/v), the mixture was centrifuged at  $15,000 \times g$  for 5 min. The resulting pellet was washed twice with ethyl acetate:EtOH (1:1, v/v). Then, the washed pellet was reconstituted with 6 M guanidine in a 20 mM  $\text{KH}_2\text{PO}_4$  buffer (pH 2.3) and centrifuged at  $15,000 \times g$  for 5 min. The absorbance of the resulting solution was measured at 370 nm.

The carbonyl content was calculated from the absorbance data, using as absorption coefficient for dinitrophenylhydrazine  $\epsilon = 22,000 \text{ M}^{-1} \text{ cm}^{-1}$ , and expressed as nmol carbonyls/mg protein. Because of the numerous washing steps, protein

**Table 2 – Effects of 2-benzazepine nitrones on 6-OHDA-induced oxidative stress in brain mitochondria**

Compound	$\text{IC}_{50}$ ( $\mu\text{M}$ )		Lipophilicity	
	LPO (TBARS)	PCOs	$\text{clog } P^a$	$\text{log } k'_w{}^b$
PBN	8500 $\pm$ 400	11,300 $\pm$ 182	1.25	
3	374 $\pm$ 27*	97 $\pm$ 9.4*	2.30	2.41
4	176 $\pm$ 11 <sup>§</sup>	40 $\pm$ 3.4 <sup>§</sup>	2.84	2.72
5	– <sup>c</sup>	– <sup>c</sup>	3.88	3.38
6	310 $\pm$ 11*	349 $\pm$ 14 <sup>§</sup>	4.42	3.37
7	137 $\pm$ 16 <sup>§</sup>	70 $\pm$ 7.8*	3.97	3.43
8	160 $\pm$ 8.1 <sup>§</sup>	144 $\pm$ 9.3 <sup>§</sup>	3.37	3.51
9	36 $\pm$ 6.2 <sup>§</sup>	53 $\pm$ 3.9 <sup>§</sup>	2.78	3.05
10	43 $\pm$ 2.9 <sup>§</sup>	91 $\pm$ 5.7*	3.34	3.55
11	20 $\pm$ 3.5 <sup>§</sup>	48 $\pm$ 4.0 <sup>§</sup>	3.88	3.47
12	– <sup>c</sup>	184 $\pm$ 14 <sup>§</sup>	4.92	3.41

In vitro protective effects of nitrones against 6-OHDA autoxidation-dependent lipid peroxidation (LPO), as assessed by TBARS assay, and protein oxidative damage, as assessed by measuring the content of protein carbonyls (PCOs), in rat brain mitochondrial preparations.  $\text{IC}_{50}$  values, determined using the 20-min time point, are means  $\pm$  S.E.M. from four independent determinations. Statistical significance at  $P < 0.05$  (one-way ANOVA and Bonferroni test) was established in comparison with the corresponding control: \*, PBN; <sup>§</sup>, cmpd 3.

<sup>a</sup> Log of *n*-octanol-water partition coefficient calculated with the ACDLabs software, release 9.0 (Advanced Chemistry Development, Inc., Toronto, Canada).

<sup>b</sup> Log of RP-HPLC polycratic capacity factor, i.e., capacity factor extrapolated at 100% aqueous mobile phase.

<sup>c</sup> No statistically significant inhibition activity was attained up to the maximum tested concentration (1 mM).

content in the final pellet was estimated on an HCl blank pellet processed simultaneously, using a BSA standard curve in 6 M guanidine, and reading the absorbance at 280 nm [44]. The  $\text{IC}_{50}$  values are listed in Table 2.

## 2.7. Statistical analysis

Data are expressed as mean  $\pm$  S.E.M. Differences between means were statistically evaluated using the one-way ANOVA followed by the Bonferroni test. Normality of populations and homogeneity of variances were tested before each ANOVA. The accepted level of significance in all cases was  $P < 0.05$ .

## 2.8. Determination of lipophilicity parameters by RP-HPLC

The lipophilicity of the 2-benzazepine nitrone derivatives was determined by a reversed-phase HPLC method [45,46]. Compounds were dissolved in MeOH at 0.25 mg/mL, injected onto a Symmetry C18 column (15 cm  $\times$  3.9 mm i.d., 5  $\mu\text{m}$  particles) from Waters Assoc. (Milford, MA, USA), and retention data measured at regular increments of the volume fraction of methanol in pH 5.0 acetate buffer (40 mM). All the measurements were made at temperature of  $25 \pm 1$  °C, flow-rate of 1.0 mL/min and at 254 nm wavelength, on a Waters HPLC 1525 multisolvent delivery system, equipped with a Waters 2487 variable wavelength UV detector (Waters Assoc., Milford, MA, USA).

Capacity factors ( $k'$ ) of each compound at different mobile phase compositions (0.05-increments of MeOH volume frac-

tion, ranging between 0.7 and 0.3) were calculated as:  $k' = (t_R - t_0)/t_0$ , where  $t_R$  is the retention time of the solute and  $t_0$  is the column dead time, measured as the elution time of MeOH. In all the cases, the  $\log k'$  values increased with decreasing MeOH volume fraction. Linear regression analysis ( $r^2 > 0.96$ ) was performed on at least five data points (the lowest MeOH concentrations) for each compound and the linear relationship extrapolated to 100% aqueous mobile phase to yield  $\log k'_w$  values.

Lipophilicity was also computationally assessed with the ACDLabs software, release 9.0 (Advanced Chemistry Development, Inc., Toronto, Canada). Both, computational and experimental lipophilicity values are listed in Table 2.

### 3. Results

The effects of the examined 2-benzazepine nitrones (Fig. 2) on the  $\cdot\text{OH}$  generated during 6-OHDA ( $10 \mu\text{M}$ ) autoxidation were assessed by measuring the relative fluorescence after 10 min incubation time, using THA as a chemical dosimeter [14,40,42,43], and the maximal relative fluorescence ( $\Delta F_{\text{max}}$ ) was taken as a measure of  $\cdot\text{OH}$  production. Fig. 3 shows a typical recording of  $\cdot\text{OH}$  formation in the absence (control) and presence of the reference compound PBN, the most simple 2-benzazepine 2-oxide within the series (3), taken as the positive control, and the spiro C-3 cyclopentyl analog (9), behaving as the most effective compound in this assay. The  $\text{IC}_{50}$  values determined for the whole nitron set are listed in Table 1.

In line with expectations, all the 7-membered ring nitrones inhibited 6-OHDA-dependent  $\cdot\text{OH}$  formation more potently than PBN. The analog 9, ( $\pm$ )-5-methyl-4,5-dihydrospiro[2-benzazepine-3,1'-cyclopentane] 2-oxide, proved to be the most active one ( $\text{IC}_{50} = 7 \mu\text{M}$ ), displaying more than 100-fold

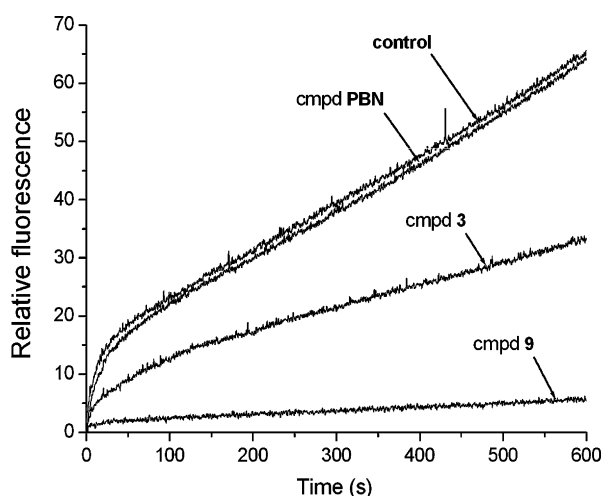


**Fig. 3** – Representative recording of  $\cdot\text{OH}$  formation during the autoxidation of 6-OHDA in the absence (control) and presence of PBN and two 2-benzazepine nitrones (3 and 9). Incubations were performed in a 25 mM phosphate buffer (pH 7.5) at 37 °C. The concentrations used were: 10  $\mu\text{M}$  for 6-OHDA and 50  $\mu\text{M}$  for the nitrones. The  $\cdot\text{OH}$  formation is monitored by the fluorescence detected using terephthalic acid as a chemical dosimeter.

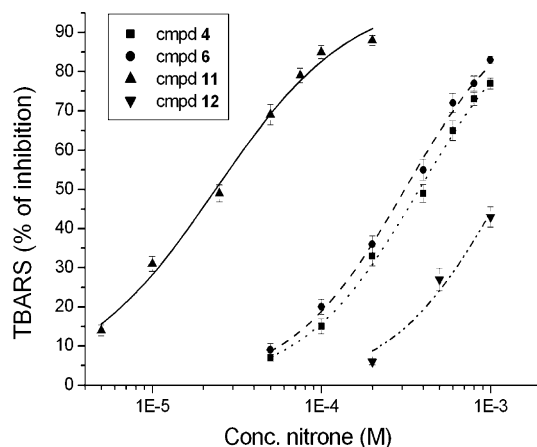


**Fig. 4** – The effects of 2-benzazepine nitrones 4, 6, 11 and 12 on the LPO induced by 6-OHDA ( $10 \mu\text{M}$ ) autoxidation in rat brain mitochondria. LPO was assessed by monitoring the TBARS formation after incubation of mitochondrial preparations ( $1 \text{ mg/mL}$ ) at 37 °C for 20 min. Data are expressed as the means  $\pm$  S.E.M. ( $n = 4$ ).

improvement over PBN. A modest, but significant, increase of the  $\cdot\text{OH}$ -scavenging activity was observed in compounds bearing 5-*gem*-dimethyl group (4, 6 and 11) compared with the respective mono-methyl derivatives (3, 5 and 10), whereas adding a methyl group to the nitron C-1 (5, 6 and 12), and to a lesser extent a phenyl group (7), decreases the reactivity of the nitron group most likely because of its limited steric accessibility.

6-OHDA-induced oxidative stress, producing significant increase of LPO product level and protein damage, is believed to be involved in neuronal cell death related to PD. Using this model, we studied the effects of the 2-benzazepine nitrones 3–12 on 6-OHDA-induced oxidative damage in rat brain mitochondrial membrane homogenates as previously described [40], assessing LPO, as measured by the formation of TBARS, and protein oxidative damage, as revealed by the PCO.

With the exceptions of compounds 5 and 12, which did not attain 50% LPO inhibition in the 5–1000  $\mu\text{M}$  concentration range, all the tested benzazepine N-oxides provoked marked reduction in the level of TBARS, showing inhibitory potencies higher than that of PBN. Inhibition was concentration dependent (Fig. 4) and  $\text{IC}_{50}$  values varied with different nitrones (Table 2).

The most simple cyclic nitron assayed (3) displayed more than 20-fold increase of LPO inhibition potency over PBN, but they were once again the spiro C-3 cycloalkyl analogs which showed the most remarkable effects with  $\text{IC}_{50}$  values of 20–43  $\mu\text{M}$  (9–11). Among them, compound 11, which bears 5-*gem*-dimethyl and C-3 spirocyclohexyl groups, behaved as the most potent one. Nitrones 5 and 12 lost LPO inhibition activity, likely due to the steric effect of  $\text{CH}_3$   $\alpha$  to N-oxide group, such an unfavorable effect being partially reversed in compounds 6 ( $R^1 = \text{methyl}$ ) and 7 ( $R^1 = \text{phenyl}$ ), thanks to the potency-increasing effects of the *gem*-dimethyl group at the C-5 position. A plot of  $\text{pIC}_{50}$  ( $-\log \text{IC}_{50}$ ) values in TBARS assay

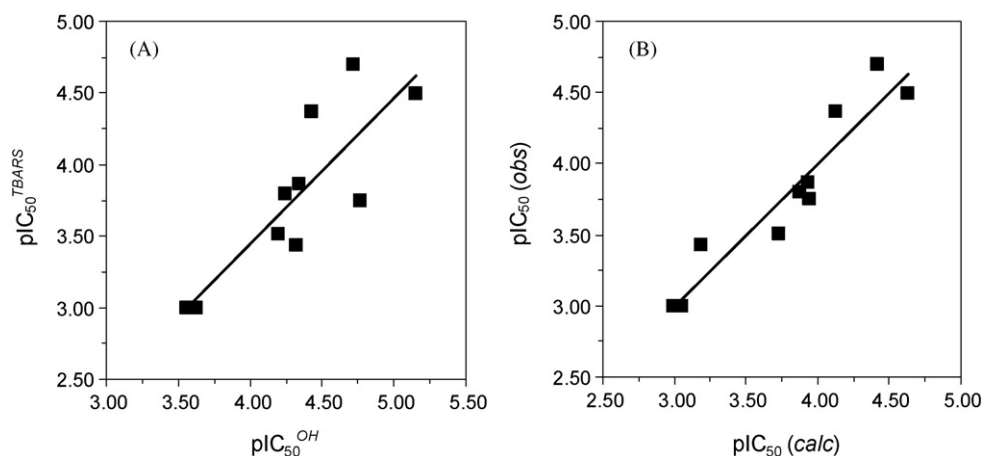


**Fig. 5 – (A) Comparison between  $\log(1/IC_{50})$  values measuring the ability of the assayed 2-benzazepine nitrones to scavenge 6-OHDA-induced  $\cdot OH$  radicals ( $pIC_{50}^{OH}$ ) and inhibit lipid peroxidation ( $pIC_{50}^{LPO}$ ) in rat brain mitochondria. (B) Plot of measured (obs) versus calculated (calc), using Eq. (3),  $pIC_{50}^{LPO}$  values.**

versus  $\cdot OH$ -scavenging activity (Fig. 5) shows that the potency of the 2-benzazepine nitrones in inhibiting LPO is reasonably correlated with their  $\cdot OH$ -scavenging ability. To allow SAR information to be retained, we used a truncated  $pIC_{50}^{LPO}$  value of 3.00 for compounds 5 and 12 ( $IC_{50} > 1$  mM), and obtained the following linear Eq. (1), which explains more than 70% of the variance in y-data:

$$pIC_{50}^{LPO} = 1.02(\pm 0.23)pIC_{50}^{OH} - 0.61(\pm 1.00) \\ n = 10, \quad r^2 = 0.711, \quad s = 0.336, \quad F = 19.6 \quad (1)$$

where  $n$  represents the number of data points,  $r^2$  the squared correlation coefficient,  $s$  the standard deviation of the regression equation,  $F$  the statistical significance of fit; 95% confidence intervals of the regression coefficients are given in parentheses.

With respect to the effect of 6-OHDA on the oxidative status of mitochondrial proteins, herein assayed by measuring the extent of PCO, PBN displayed a very low inhibitory activity ( $IC_{50} = 11.3$  mM). In contrast, the addition to the incubation of the 2-benzazepine nitrones, with the only exception of compound 5, caused significant reduction in carbonyl content in rat brain mitochondrial proteins (Table 2). The nitrone derivative 3 inhibited PCO with an  $IC_{50}$  value of 97  $\mu M$ , but compounds 4, 9 and 11 showed a 2-fold increase of the inhibitory potency over 3. PCO inhibition effects quite similar to those measured on LPO, albeit not linearly correlated to them, were observed. As a matter of fact, like in LPO inhibition, 5-*gem*-dimethyl derivatives were more potent inhibitors than the corresponding 5-methyl ones (compare 4, 6 and 11 with 3, 5 and 10, respectively), as well as  $R^1$ -methyl bearing 2-benzazepine nitrones (5, 6 and 12) loose antioxidant activity compared to the corresponding  $R^1$ -desmethyl compounds (3, 4 and 10), but in contrast with the LPO/TBARS results, in the PCO assay the spiro C-3 cyclohexyl compounds 10 and 11 did not show any remarkable increase of potency compared with the corresponding 3-*gem*-dimethyl analogs 3 and 4, respectively.

Linear regression between  $pIC_{50}$  value in PCO assay (a truncated  $pIC_{50}^{PCO}$  value of 3.00 was used, in this case, for compound 5) and  $\cdot OH$ -decreasing ability yielded the following linear Eq. (2), statistically poorer than Eq. (1):

$$pIC_{50}^{PCO} = 0.71(\pm 0.19)pIC_{50}^{OH} + 0.85(\pm 0.19) \\ n = 10, \quad r^2 = 0.640, \quad s = 0.276, \quad F = 14.2 \quad (2)$$

Taking into account the results obtained by others [31–34], who highlight a major role of lipophilicity in modulating LPO inhibition by cyclic nitrones, we determined the relative lipophilicity of the 2-benzazepine nitrones by a well-established reversed-phase (RP)-HPLC technique ( $\log k'_w$ ) [47], using previously reported methods [45,46]. A comparison between the experimental parameters  $\log k'_w$  (Table 2) and octanol-water partition coefficients calculated by the ACDLabs software ( $\log P$ ) showed that a linear relation between the two sets of lipophilicity parameters holds up to  $\log P$  of ca. 3.5, a value beyond which  $\log k'_w$  no longer increases. This should be not surprising, since the ACDLabs calculation system, as well as other  $\log P$  fragmental calculation methods, may fail in lipophilicity prediction either because of the high uncertainty of the estimated fragmental  $\log P$  values of the nitrone group and connected atoms and/or because the highest  $\log P$  values are too close or above the upper limit for precise partition coefficient measurements, which constitute the basis of the  $\log P$  calculation fragmental system. The spread of the measured  $\log k'_w$  parameters is rather limited (1.14 log units), and most of the examined compounds (5–8, 10–12) varied in just 0.2  $\log k'_w$  units, that is a too small range to be a matter of physicochemical interpretation. Nonetheless, within the limits of the small set examined, when comparing  $\log k'_w$  values among themselves, some significant findings can be highlighted. Thus, the addition of the second  $CH_3$  group at C-5 leads to a small (compare 4 with 3) to nil (compare 6 with 5) increase of lipophilicity. The increment of  $\log k'_w$  by about one unit caused by 1-methyl group (5 versus 3), and to a lesser

extent by 1-phenyl group (7 versus 4), should account for the decrease in the water-accessible surface area of the polar  $N^+-O^-$  group, besides the additive hydrophobic effect of the  $R^1$ -substituents.

Investigating the role of lipophilicity in inhibiting TBARS formation in brain mitochondria, a trend was observed which suggested a bilinear relationship [48] between  $pIC_{50}^{LPO}$  and  $\log k'_w$ . LPO inhibitory potency of 2-benzazepine nitrones increases as the  $\log k'_w$  increases from 2.41 for 3 to 3.05 for 9; when  $\log k'_w$  surpasses the value of 3.37, the potency no longer increases but steeply declines with further increase of the  $\log k'_w$ . Nonlinear regression between  $pIC_{50}^{LPO}$  and  $\log k'_w$  did not afford any statistically valid quantitative SAR, whereas including in Eq. (1) the lipophilicity parameter as a second independent variable, the following two-parameter equation was obtained, which explains 90% of the variance in the LPO inhibition data:

$$pIC_{50}^{LPO} = 1.18(\pm 0.23)pIC_{50}^{OH} + 0.70(\pm 0.19)\log k'_w - 3.61(\pm 1.04)$$

$$n = 10, \quad r^2 = 0.900, \quad s = 0.211, \quad F = 31.5 \quad (3)$$

A plot of the measured versus calculated  $pIC_{50}^{LPO}$  values is illustrated in Fig. 5. Eq. (3) shows that the inhibition potency of 6-OHDA-induced TBARS formation in rat brain mitochondria primarily depends upon the  $\bullet OH$ -scavenging activity, but significantly increases with increasing lipophilicity, as accounted for by the  $\log k'_w$  parameter. The introduction of  $\log P$  instead of  $\log k'_w$  proved to be not statistically significant. Addition of  $\log k'_w$  (and  $\log P$  as well) to Eq. (2), which describes the inhibition potency against PCO ( $pIC_{50}^{PCO}$ ), did not result in any statistical improvement, suggesting that lipophilicity does not play a role in inhibiting PCO as important as in inhibiting formation of lipid peroxide products.

#### 4. Discussion

There is growing evidence indicating that oxidative stress, which results in significant increase of lipid peroxidation products and protein oxidative damage, is a key contributor to the pathogenesis of several neurodegenerative diseases, including PD [14,49–51]. In this study, we used 6-OHDA, a neurotoxin producing experimental model of PD [52], to generate in vitro  $\bullet OH$  and to cause LPO and PCO [51], and investigated a series of new seven-membered cyclic analogs of the spin trap PBN, namely 3,3-dimethyl-4,5-dihydro-3H-2-benzazepine nitrones and their spiro C-3 cycloalkyl analogs, for their ability to protect rat brain mitochondria against oxidative injury.

Autoxidation of 6-OHDA is an important source of intracellular ROS. Under physiological conditions, it is rapidly oxidized affording formation of  $H_2O_2$ ,  $\bullet OH$ , and the corresponding *p*-quinone [53]. The formation of the hazardous  $\bullet OH$  during the autoxidation of 6-OHDA has been proven to occur without involvement of ferrous ion, or any other transition metal ion, in Fenton-type reactions [54]. The inhibition of the 6-OHDA-induced oxidative damage by our 2-benzazepine nitrones should primarily stem from their ability to trap radical species, as previously shown by others through ESR

studies on strictly related analogs [33]. Our data from a chemical fluorimetric assay using THA as  $\bullet OH$  dosimeter [42] indicate that compounds 3–12 reduce, more efficiently than does PBN, 6-OHDA-induced  $\bullet OH$  production (Table 1). They should act as  $\bullet OH$  scavengers, since in our assay conditions we can rule out iron chelation and, thus, prevention of the Fenton reaction, as instead demonstrated using other models of oxidative stress [26]. Relating structure of the 2-benzazepine nitrones examined with their activity against  $\bullet OH$  production highlighted a 2–4-fold increase effect of the *gem*-dimethyl group at C-5 (4, 6 and 11), compared with the respective monomethyl derivatives (3, 5 and 10). Such a higher activity of 5,5-dimethyl-substituted 2-benzazepine nitrones could most likely be attributed to their structural peculiarity, inasmuch the presence of the 5-*gem*-dimethyl group should flatten the azepine ring, thus enhancing reactivity (radical attack onto nitron fragment taking place from both sides of the azepine *pseudo* plane) and/or increasing stability of the resulting spin adducts [33]. The  $^1H$  NMR data of the 5-*gem*-dimethyl derivatives, in agreement with geometry calculations on optimized structures, are reasonably consistent with this assumption. Indeed, the 4- $CH_2$  protons, which lose their axial and equatorial characters, resonate as singlet, showing their equivalence in the 5-*gem*-dimethyl-bearing derivatives 4, 6 and 11. In contrast, in 5-methyl derivatives 3, 5 and 10 the C-4 protons' signals appear as two distinct doublets of doublets, with characteristic coupling constants for the coupling with the vicinal H-5, indicating that, in solution, the azepine ring preferably adopts a chair conformation with the methyl group at C-5 disposed equatorially [35]. As an additional SAR information, a methyl group to the nitron C-1 (5, 6 and 12), and to a lesser extent a phenyl group (7), diminish the  $\bullet OH$ -scavenging activity of the nitron group, because of its limited steric accessibility.

Mitochondria-specific effects, potentially contributing to neuroprotective properties, were determined as the ability of the examined 2-benzazepine nitrones to inhibit LPO and PCO (Table 2), induced in rat brain mitochondria by autoxidation of 6-OHDA. Our data showed that the investigated cyclic nitrones are one-two orders of magnitude more potent than PBN in protecting rat brain mitochondria against the oxidative insults, as measured by inhibition of TBARS formation (LPO) and PCO increase. The  $IC_{50}$  values determined in both assays are somehow correlated with the ability of the 2-benzazepine nitrones to scavenge  $\bullet OH$  radicals (Eqs. (1) and (2)), suggesting that their neuroprotective activity may stem primarily, but not uniquely, from trapping these damaging radicals. Formation of nitrosyl radical species, which act as chain-breaking antioxidants [55], preventing propagation of both LPO and PCO, may be supposed as an additional mechanism accounting for the observed protective properties.

From an SAR point of view,  $R^1$  substitution with a methyl group appears as unfavorable, whereas the presence of the 5-*gem*-dimethyl group, more than the 5-methyl one, as well as the replacement of the 3-*gem*-dimethyl group with a spirocyclopentyl or spirocyclohexyl moiety, increases the inhibition potency against both LPO and PCO. A statistically significant equation (Eq. (3)) was derived, that correlates the in vitro LPO (but not PCO) inhibition data with  $\bullet OH$ -scavenging reactivity and lipophilicity of the 2-benzazepine nitrones, as

described by the experimental  $\log k'_w$  parameter (but not by the calculated  $\log P$ ). According to other reported quantitative SARs [31], Eq. (3) indicates that, their  $\cdot\text{OH}$ -scavenging potency being equal, 2-benzazepine nitrones having higher affinity for and greater residence time in the lipid phase are more effective in protecting the lipids from peroxidation. Among the most potent nitrones examined so far, compound 11 is noteworthy and is expected to be suitable for replacing PBN, whose oxygen-centered radical spin adducts are very short-lived [56], in the investigation of radicals in lipid membranes.

Investigating some systematic variations in the structure of 3,3-dimethyl-4,5-dihydro-3H-2-benzazepine N-oxide, some new cyclic nitrones have been singled out for their promising activity in protecting rat brain mitochondria from oxidative injury triggered by the PD-inducing neurotoxin 6-OHDA. Some of the examined derivatives, especially compound 11, which incorporates into its structure the best features identified in this study (5-*gem*-dimethyl group and spiro C-3 cyclohexyl groups, and optimal lipophilicity), proved to be orders of magnitude more effective than PBN in vitro against 6-OHDA-induced mitochondrial lipid peroxide formation and protein oxidative damage.

The SAR information and lipophilicity data reported herein are important for drug design of potential therapeutics useful for treatment of neurodegenerative conditions in which oxidative stress plays a role. Nevertheless, other properties must be taken into account for improving their therapeutic index. Indeed, while lipophilicity is generally recognized as a major property modulating antioxidant activity of cyclic nitrones in both LPO assay and maintenance of cell viability in models of oxidative injury in vitro [26,57], brain penetration and toxicity to neurons (ranging from sedation at moderate doses to death at very high doses), which in turn did not appear to linearly depend on lipophilicity and nitrone brain level following ip injection in rats, respectively, strongly contribute to the therapeutic utility of cyclic nitrones in neurodegenerative disorders [57]. Results from our current investigation on selected 2-benzazepine nitrones in cell cultures and in vivo models of oxidative stress are expected to shed light on physicochemical properties of nitrone derivatives which could readily penetrate the brain while retaining a desirable side effect profile.

## Acknowledgements

The Spanish authors thank the Ministerio de Educación y Ciencia and the Europe Regional Development Fund (Madrid, Spain, Grants BFI2003-00493 and SAF2007-66114) for financial support. The Italian authors thank the Italian Ministry for Education Universities and Research (MIUR, Rome, Italy; PRIN 2004, Grant No. 2004037521\_006) for financial support.

## REFERENCES

- [1] Yung LM, Leung FP, Yao X, Chen ZY, Huang Y. Reactive oxygen species in vascular wall. *Cardiovasc Hematol Disord Drug Targets* 2006;6:1–19.
- [2] Geronikaki AA, Gavalas AM. Antioxidants and inflammatory disease: synthetic and natural antioxidants with anti-inflammatory activity. *Comb Chem High Throughput Screen* 2006;9:425–42.
- [3] Mandel S, Grünblatt E, Riederer P, Gerlach M, Levites Y, Youdim MBH. Neuroprotective strategies in Parkinson's disease: an update on progress. *CNS drugs* 2003;17:729–62.
- [4] Stadtman ER. Protein oxidation and aging. *Free Radic Res* 2006;40:1250–8.
- [5] Simola N, Morelli M, Carta AR. The 6-hydroxydopamine model of Parkinson's disease. *Neurotox Res* 2007;11:151–67.
- [6] Smeyne RJ, Jackson-Lewis V. The MPTP model of Parkinson's disease. *Mol Brain Res* 2005;134:57–66.
- [7] Lorenc-Koci E, Rommelspacher H, Schulze G, Wernicke C, Kuter K, Smiałowska M, et al. Parkinson's disease-like syndrome in rats induced by 2,9-dimethyl-beta-carbolinium ion, a beta-carboline occurring in the human brain. *Behav Pharmacol* 2006;17:463–73.
- [8] McNaught KStP, Carrupt P-A, Altomare C, Cellamare S, Carotti A, Testa B, et al. Isoquinoline derivatives as endogenous neurotoxins in the aetiology of Parkinson's disease. *Biochem Pharmacol* 1998;56:921–33.
- [9] Grünblatt E, Mandel S, Youdim MB. Neuroprotective strategies in Parkinson's disease using the models of 6-hydroxydopamine and MPTP. *Ann NY Acad Sci* 2000;899:262–73.
- [10] McDowell I. Alzheimer's disease: insights from epidemiology. *Aging* 2001;13:143–62.
- [11] Cadet JL, Katz M, Jackson-Lewis V, Fahn S. Vitamin E attenuates the toxic effects of intrastratial injection of 6-hydroxydopamine (6-OHDA) in rats: behavioral and biochemical evidence. *Brain Res* 1989;476:10–5.
- [12] Kaur D, Yantiri F, Rajagopalan S, Kumar J, Mo JQ, Boonplueang R, et al. Genetic or pharmacological iron chelation prevents MPTP-induced neurotoxicity in vivo: a novel therapy for Parkinson's disease. *Neuron* 2003;37:899–909.
- [13] Zecca L, Youdim MB, Riederer P, Condor JR, Crichton RR. Iron, brain ageing and neurodegenerative disorders. *Nat Rev Neurosci* 2004;5:863–73.
- [14] Soto-Otero R, Méndez-Álvarez E, Hermida-Ameijeiras Á, López-Real AM, Labandeira-García JL. Effects of (–)-nicotine and (–)-cotinine on 6-hydroxydopamine-induced oxidative stress and neurotoxicity: relevance for Parkinson's disease. *Biochem Pharmacol* 2002;64:125–35.
- [15] Pezzella A, d'Ischia M, Napolitano A, Misuraca G, Prota G. Iron-mediated generation of the neurotoxin 6-hydroxydopamine quinone by reaction of fatty acid hydroperoxides with dopamine: a possible contributory mechanism for neuronal degeneration in Parkinson's disease. *J Med Chem* 1997;40:2211–6.
- [16] Graham DG, Tiffany SM, Bell Jr WR, Gutknecht WF. Autoxidation versus covalent binding of quinones as the mechanism of toxicity of dopamine, 6-hydroxydopamine, and related compounds toward C1300 neuroblastoma cells in vitro. *Mol Pharmacol* 1978;14:644–53.
- [17] Gee P, Davison AJ. Intermediates in the aerobic autoxidation of 6-hydroxydopamine: relative importance under different reaction conditions. *Free Radic Biol Med* 1989;6:271–84.
- [18] Glinka YY, Youdim MBH. Inhibition of mitochondrial complexes I and IV by 6-hydroxydopamine. *Eur J Pharmacol* 1995;292:329–32.
- [19] Glinka YY, Tipton KF, Youdim MBH. Nature of inhibition of mitochondrial respiratory complex I by 6-hydroxydopamine. *J Neurochem* 1996;66:2004–10.
- [20] Kumar R, Agarwal AK, Seth PK. Free radical-generated neurotoxicity of 6-hydroxydopamine. *J Neurochem* 1995;64:1703–7.

- [21] Dalle-Donne I, Aldini G, Carini M, Colombo R, Rossi R, Milani A. Protein carbonylation, cellular dysfunction, and disease progression. *J Cell Mol Med* 2006;10:389–406.
- [22] Dobson CM. Protein folding and misfolding. *Nature* 2003;426:884–90.
- [23] Aldini G, Dalle-Donne I, Facino RM, Milani A, Carini M. Intervention strategies to inhibit carbonylation by lipoxidation-derived reactive carbonyls. *Med Res Rev* 2006;27:817–68.
- [24] Choi J, Rees HD, Weintraub ST, Levey AI, Chin LS, Li L. Oxidative modifications and aggregation of Cu/Zn superoxide dismutase associated with Alzheimer's and Parkinson's diseases. *J Biol Chem* 2005;280:11648–55.
- [25] Thomas CE, Huber EW, Ohlweiler DF. Hydroxyl and peroxy radical trapping by the monoamine oxidase-B inhibitors deprenyl and MDL 72,974A: implications for protection of biological substrates. *Free Radic Biol Med* 1997;22:733–7.
- [26] Thomas CE, Ohlweiler DF, Taylor VL, Schmidt CJ. Radical trapping and inhibition of iron-dependent CNS damage by cyclic nitron spin traps. *J Neurochem* 1997;68:1173–82.
- [27] Maples KR, Ma F, Zhang YK. Comparison of the radical trapping ability of PBN, S-PPBN and NXY-059. *Free Radic Res* 2001;34:417–26.
- [28] Wang CX, Shuaib A. NXY-059: a neuroprotective agent in acute stroke. *Int J Clin Pract* 2004;58:964–9.
- [29] Carney JM, Starke-Reed PE, Oliver CN, Landum RW, Cheng MS, Wu JF, et al. Reversal of age-related increase in brain protein oxidation, decrease in enzyme activity, and loss in temporal and spatial memory by chronic administration of the spin trapping compound *N*-tert-butyl- $\alpha$ -phenylnitron. *Proc Natl Acad Sci USA* 1991;88:3633–6.
- [30] Chen Q, Fischer A, Reagan JD, Yan L-J, Ames BN. Oxidative DNA damage and senescence of human diploid fibroblast cells. *Proc Natl Acad Sci USA* 1995;92:4337–41.
- [31] Fevig TL, Bowen SM, Janowick DA, Jones BK, Munson HR, Ohlweiler DF, et al. Design, synthesis and in vitro evaluation of cyclic nitrones as free radical traps for the treatment of stroke. *J Med Chem* 1996;39:4988–96.
- [32] Bernotas RC, Thomas CE, Carr AA, Nieduzak TR, Adams GA, Ohlweiler DF, et al. Synthesis and radical scavenging activity of 3,3-dialkyl-3,4-dihydroisoquinoline 2-oxides. *Bioorg Med Chem Lett* 1996;6:1105–10.
- [33] Thomas CE, Ohlweiler DF, Kalyanaraman B. Multiple mechanisms for inhibition of low density lipoprotein oxidation by novel cyclic nitron spin traps. *J Biol Chem* 1994;269:28055–61.
- [34] Thomas CE, Ohlweiler DF, Carr AA, Nieduzak TR, Hay DA, Adams G, et al. Characterization of the radical trapping activity of a novel series of cyclic nitrones spin traps. *J Biol Chem* 1996;271:3097–104.
- [35] Varlamov A, Kouznetsov V, Zubkov F, Chernyshev A, Alexandrov G, Palma A, et al. Efficient synthesis and spectroscopic analysis of 8-nitro spiro C-3-annulated 2-benzazepines and their N-oxides. *Synthesis* 2001;6: 849–54.
- [36] Vargas Méndez LY, Kouznetsov V. 4-N-Aryl(benzyl)amino-4-heteroaryl-1-butenes as building blocks in heterocyclic synthesis. 3. A simple synthesis of fluorinated 4-methyl-2-(3-pyridyl)-1,2,3,4-tetrahydroquinolines and their respective quinolines. *Heterocycl Commun* 2002;8: 583–6.
- [37] Urbina JMG, Cortés JC, Palma A, López SN, Zacchino SA, Enriz DR, et al. Inhibitors of the fungal cell wall. Synthesis of 4-aryl-4-N-arylamine-1-butenes and related compounds with inhibitory activities on  $\beta$  (1-3) glucan and chitin synthases. *Bioorg Med Chem* 2000;8:691–8.
- [38] Puentes CO, Kouznetsov V. Recent advancements in the homoallylamine chemistry. *J Heterocyclic Chem* 2002;39:595–614.
- [39] Kouznetsov VV, Palma AR, Salas S, Vargas LY, Zubkov FI, Varlamov AV, et al. Chemistry of functionalized benzazepines. 5. Synthesis and chemical transformation of the 1,2,4,5-tetrahydrospiro[3H-2-benzazepin-3,1'-cycloalkanes]. *J Heterocyclic Chem* 1997;34: 1591–5.
- [40] Hermida-Ameijeiras Á, Méndez-Álvarez E, Sánchez-Iglesias S, Sanmartín-Suárez C, Soto-Otero R. Autoxidation of MAO-mediated metabolism of dopamine as a potential cause of oxidative stress: sole of ferrous and ferric ions. *Neurochem Int* 2004;45:103–16.
- [41] Markwell MAK, Haas SM, Bieber LL, Tolbert NE. A modification of the Lowry procedure to simplify protein determination in membrane and lipoprotein samples. *Anal Biochem* 1978;87:206–10.
- [42] Barreto JC, Smith GS, Strobel NH, McQuillin PA, Miller TA. Terephthalic acid: a dosimeter for the detection of hydroxyl radicals in vitro. *Life Sci* 1995;56:PL89–96.
- [43] Soto-Otero R, Sanmartín-Suárez C, Sánchez-Iglesias S, Hermida-Ameijeiras A, Sánchez-Sellero I, Méndez-Álvarez E. Study on the ability of 1,2,3,4-tetrahydropapaveroline to cause oxidative stress: mechanisms and potential implications in relation to Parkinson's disease. *J Biochem Mol Toxicol* 2006;20:209–20.
- [44] Reznick AZ, Packer L. Oxidative damage to proteins: spectrophotometric method for carbonyl assay. *Methods Enzymol* 1994;233:357–63.
- [45] de Candia M, Fossa P, Cellamare S, Mosti L, Carotti A, Altomare C. Insights into structure–activity relationships from lipophilicity profiles of pyridin-2(1H)-one analogs of the cardiotoxic agent milrinone. *Eur J Pharm Sci* 2005;26:78–86.
- [46] De Marco A, de Candia M, Carotti A, Cellamare S, De Candia E, Altomare C. Lipophilicity-related inhibition of platelet aggregation by nipecotic acid anilides. *Eur J Pharm Sci* 2004;22:153–64.
- [47] Braumann T. Determination of hydrophobic parameters by reversed-phase liquid chromatography: theory, experimental technique, and application in studies on quantitative structure–activity relationships. *J Chromatogr* 1986;373:191–225.
- [48] Kubinyi H. Quantitative models. In: Mannhold R, Krogsgaard-Larsen P, Timmerman H, editors. QSAR: Hansch analysis and related approaches. Weinheim: VCH Verlagsgesellschaft mbH; 1993. p. 68–77.
- [49] Alam ZI, Daniel SE, Lees AJ, Marsden DC, Jenner P, Halliwell P. A generalized increase in protein carbonyl in the brain in Parkinson's disease but not incidental Lewy body disease. *J Neurochem* 1997;69:1326–9.
- [50] Dexter DT, Holley AE, Flitter WE, Slater TF, Wells FR, Daniel SE, et al. Increased levels of lipid hydroperoxides in the parkinsonian substantia nigra: an HPLC and ESR study. *Mov Disord* 1994;9:92–7.
- [51] Sánchez-Iglesias S, Rey P, Méndez-Álvarez E, Labandeira-García JL, Soto-Otero R. Time-course of brain oxidative damage caused by intrastratial administration of 6-hydroxydopamine in a rat model of Parkinson's disease. *Neurochem Res* 2007;32:99–105.
- [52] Dauer W, Przedborski S. Parkinson's disease: mechanisms and models. *Neuron* 2003;39:889–909.
- [53] Soto-Otero R, Méndez-Álvarez E, Hermida-Ameijeiras A, Muñoz-Patiño A, Labandeira-García JL. Autoxidation and neurotoxicity of 6-hydroxydopamine in the presence of some antioxidants: potential implication in relation to the pathogenesis of Parkinson's disease. *J Neurochem* 2000;74:1605–12.
- [54] Méndez-Álvarez E, Soto-Otero R, Hermida-Ameijeiras A, López-Martín ME, Labandeira-García JL. Effect of iron and

- manganese on hydroxyl radical production by 6-hydroxydopamine: mediation of antioxidants. *Free Radic Biol Med* 2001;31:986–98.
- [55] Skolimowski J, Kochman A, Gębicka L, Metodiewa E. Synthesis and antioxidant activity evaluation of novel antiparkinsonian agents, aminoadamantane derivatives of nitroxyl free radical. *Bioorg Med Chem* 2003;11:3529–39.
- [56] Janzen EG, Kotake Y, Hinton RD. Stabilities of hydroxyl radical spin adducts of PBN-type spin traps. *Free Radic Biol Med* 1992;12:169–73.
- [57] Thomas CE, Bernardelli P, Bowen SM, Chaney SF, Friedrich D, Janowick DA, et al. Cyclic nitron free radical traps: Isolation, Identification, and synthesis of 3,3-dimethyl-3,4-dihydroisoquinolin-4-ol N-oxide, a metabolite with reduced side effects. *J Med Chem* 1996;39:4997–5004.